GPS CLOCKS IN SPACE: CURRENT PERFORMANCE AND PLANS FOR THE FUTURE

Mr. Todd Dass, Mr. Gerald Freed, Mr. John Petzinger, Dr. John Rajan
ITT Industries
Aerospace/Communications Division, NJ Engineering Center
100 Kingsland Rd., Clifton, NJ 07014-1993, USA
John.Rajan@ITT.com
Tel: +1 973 284 4835; Fax: +1 973 284 3394

Mr. Thomas J. Lynch and Mr. John Vaccaro
PerkinElmer Optoelectronics
35 Congress St., Salem, MA 01970-0662, USA
Tel: +1 978 745 3200

Abstract

The ITT Industries-developed GPS IIR satellite payloads have been on-orbit since 1997, providing outstanding signal-in-space performance. Much of credit for this outstanding performance can be given to the GPS IIR Time Keeping System (TKS) and the GPS-IIR spacecraft bus, which keeps the payload in a mechanically and thermally stable condition. A key component of the TKS system is PerkinElmer's rubidium atomic frequency standard (RAFS). We now have a grand total of 15 years of on-orbit experience with the GPS IIR TKS and RAFS. In this paper we will present the current on-orbit performance of GPS IIR TKS and RAFS. Since GPS IIR, ITT and PerkinElmer have made significant performance enhancements to the TKS and RAFS. This paper will highlight performance of the next generation TKS with the enhanced RAFS (ERAFS) and an improved **precision phase meter** ***(PPM).***

The paper discusses current on-orbit performance of the GPS IIR TKS and RAFS and shows that they match expectations. The paper also discusses the modifications that comprise the ERAFS and associated performance improvement over the legacy RAFS. Finally, the paper discusses potential performance enhancements for the next generation TKS.

INTRODUCTION

A block diagram of the GPS Block IIR Time Keeping System (TKS) is shown in Figure 1. The source of the Block IIR signal timing for a given satellite is the onboard *rubidium atomic frequency standard*, which we refer to as the RAFS. For redundancy, there are three RAFS in the TKS, one is active and two are backups. The RAFS is a free-running clock at approximately 13.4 MHz, with no controls. The 13.4 MHz signal is passed through the onboard TKS, which phase locks a voltage-controlled crystal oscillator (VCXO) to it to generate a 10.23 MHz transmitted clock, which is sent to all the GPS users as an L-band signal. The 10.23 MHz signal can be adjusted in phase, frequency, and frequency drift by commands sent to the TKS from ground control. GPS user equipment can compute GPS Time from a given satellite by correcting the satellite's transmitted time by the clock residuals broadcast in the L-band Navigation Message.

This paper will show the on-orbit performance of the GPS IIR TKS/RAFS. To put the IIR into perspective, performance data from GPS II/IIA will be included. We will present both the factory-measured and on-orbit frequency stability, as well as the actual navigation performance achieved from each SV over more than a year. We will show that the navigation performance follows the RAFS stability. In addition, we will show the factory-measured stability on the remaining IIR SVs on the ground, which gives perspective on the expected future on-orbit performance of a GPS IIR-dominated constellation.

CURRENT GPS IIR ON-ORBIT PERFORMANCE

The Master Control Station uploads each GPS satellite daily. Among other things, the GPS IIR upload contains a 210-day prediction of satellite clock residuals. The GPS satellite broadcasts these residuals to the users in the L-band signal. Since the upload occurs daily, the age of the broadcast clock residuals is zeroed roughly every 24 hours. It follows that the performance of a given GPS satellite is highly dependent on the stability of its atomic clock, particularly the stability at 1 day.

Figure 2 shows a ranking of GPS clocks by frequency stability at 1 day for the first quarter of 2002. The SV with the most stable clocks contain rubidium atomic frequency standards. The five most stable clocks are the GPS IIR PerkinElmer RAFS on SVNs 41, 43, 46, 51, and 54. The RAFS on SVN 44 appears to be out of character from the other five GPS IIR RAFS.

Estimated range deviation (ERD) is defined to be the difference between the predicted ephemeris/clock and the Master Control Station (MCS) Kalman filter current state estimate rms'd over a continuum of geodetic locations visible to the SV. Figure 3 contains plots of the maximum ERD for all the GPS IIR for every day in the period from January 2001 through April 2002. In these plots, ERD is dominated by the stability of the RAFS. As expected, the most stable clocks have the best ERD performance. The outliers visible in the ERD plots for SVNs 41, 46, 51, and 54 were caused by random frequency breaks of 10^{-13} magnitude in the RAFS. In addition, the early data for SVN 54 show MCS Kalman filter convergence during beginning of life RAFS frequency stabilization. Figure 4 and Figure 5 contain the ERD plots for all the GPS II/IIA during the same time period for comparison purposes.

Figure 6 contains a plot of the frequency stability at 1-day measured by PerkinElmer before delivery to ITT Industries. The GPS IIR has three RAFS per SV. The plot shows the stability of the RAFS in each slot on each SV. The least stable RAFS of the lot is in slot 2 of SVN 44, which is the currently active clock on that SV. Therefore, the ERD plot for SVN 44 likely sets the standard for the worst-case performance for any IIR SV. Figure 7 is a plot comparing the on-orbit frequency stability at 1 day to the stability measured by PerkinElmer during Factory Acceptance Testing. This plot shows that the PerkinElmer data are a good predictor of on-orbit performance.

ERAFS

The stability specification for the PerkinElmer RAFS-IIR rubidium standard is $\sigma_y(\tau) \leq 3\times10^{-12}/\sqrt{\tau}+5\times10^{-14}$. This places an upper stability limit of $\sigma_y \leq 6\times10^{-14}$ at an averaging time of 1 day on the RAFS-IIR. Five of the six RAFS-IIR standards now in service have significantly better performance than the current requirement. This has had the effect of raising performance expectations of the overall system and highlighted the poorer performance of RAFS-IIR SN 009, currently in service on board SVN 44. RAFS-IIR SN 009's factory test data were near the upper limit of $\sigma_y \leq 6\times10^{-14}$ at shipment, and this RAFS has exhibited out-of-specification performance in service.

The overall excellent performance of the PerkinElmer RAFS-IIR has also drawn attention to frequency jumps or breaks. Features as small as 5×10^{-14} are observable because of the low noise of the RAFS. Frequency jumps or breaks of various magnitudes, some quasi-periodic in nature have been attributed to the in-service RAFSs. Some frequency breaks have been large enough to require ground intervention.

RAFS SN 009 is exhibiting both out-of-character stability at averaging times in the range of about one-half of a day and longer and frequency breaks in the range of up to $6pp10^{13}$. Although to date the frequency breaks attributed to SN 009 have not been an operational concern, the overall stability of SN 009 has generated interest in improving the existing available RAFSs in both regards.

The good correlation between the on-orbit frequency data and acceptance test frequency data, and acceptance test experience with approximately 80 RAFS-IIR and RFS-IIF standards produced by PerkinElmer, provide a means to diagnose a likely cause of SN 009's deficient stability. The likely cause is the rubidium lamp.

Although not the overriding issue with RAFS-IIR SN009, there is considerable history to indicate that frequency jumps or breaks are also related to the rubidium lamp.

An attractive means to improve or upgrade the overall stability performance of the RAFS does exist and is being used in thousands of tactical rubidium standards such as the PerkinElmer RFS-10 and in the PerkinElmer RFS-IIF for the GPS IIF program. The improvement is based on lower noise of the detected rubidium signal. A RAFS that is upgraded in such a way is referred to as an *enhanced RAFS* or ERAFS.

A significant driver of the overall stability performance of the RAFS-IIR is the rubidium signal-to-noise (S/N) ratio **[1]**. The noise component in this ratio is in large part due to shot noise generated by unused or excess light that reaches the photo detector. In the RAFS-IIR, the krypton buffer gas used in the rubidium lamp is the greatest contributor to this noise effect. Optical filtering can be effective in reducing the amount of unused light reaching the photo detector.

Although optical filtering techniques can be very effective, in the case of a krypton buffer gas rubidium lamp, the spectral lines of the buffer gas light are interspersed with the rubidium spectral lines that are used for optical pumping in the absorption cell. This makes optical filtering impractical in the case of a krypton buffer gas lamp. The relative location of the krypton and rubidium spectral lines is shown in Figure 8.

Fortunately an alternative to krypton, xenon in conjunction with spectral filtering improves the S/N ratio. As shown in Figure 9, xenon buffer gas spectral lines are spaced far enough from rubidium spectral lines to make optical filtering possible. The placement of an optical filter in the light path is very effective in preventing the xenon buffer gas spectra from reaching the photo detector and generating undesirable shot noise. The PerkinElmer ERAFS physics package is shown in Figure 10.

When xenon buffer gas lamp and spectral filtering methods are employed, the S/N ratio is improved from 75 dB to 87 dB. Taking other dominant noise effects into account, a 2:1 improvement in the overall stability results. In the ERAFS this results in an improvement in the calculated Allan deviation from approximately $2\times10^{-12}/\sqrt{\tau}$ to $1\times10^{-12}/\sqrt{\tau}$. Test data from an RAFS with a krypton buffer gas lamp and an ERAFS with a xenon buffer gas lamp and spectral filtering is shown in Figure 11.

Certain minor adjustments to the ERAFS preamplifier and servo are required in conjunction with the improvements.

The cause of frequency breaks is not fully understood. Although most breaks are likely a result of lamp phenomena, one cannot draw a conclusion that the lamp is the only cause of frequency breaks.

Over the past several years PerkinElmer has made progress in the area of random frequency breaks that have been observed in the on-orbit RAFS. Features as small as $5pp10^{14}$ are observable because of the low noise of the RAFS. Through tightened process controls and careful selection of rubidium lamps, frequency breaks have become much less pervasive during acceptance testing of RAFS (IIR) and RFS (IIF) rubidium standards. A change to xenon buffer gas and including a spectral filter alone are not expected to have any influence on frequency breaks. However, upgrading the available RAFSs with xenon lamps that have been subjected to processing improvements will result in improved overall performance and a lower probability of frequency breaks.

One should keep in mind that the acceptance test of these units includes a relatively short aging period of 30 days, during which time the stability performance is closely monitored. This is extremely short in comparison to the expected long life (approximately 10 years) of these units. Considering the variety of breaks reported with various points of inception, periodicity, and size, it is unwise to conclude that the issue has been completely resolved.

NEXT GENERATION TKS PERFORMANCE GOAL AND COMPONENTS

Up to this point we have only discussed one component of the TKS, the RAFS, and shown that the enhanced RAFS (ERAFS) should result in an improvement in long-term stability of the GPS timing signal and fewer frequency breaks. Our performance goal for a next-generation TKS is a 10:1 improvement in timing stability across the entire range of 1s to 10^5 seconds, and also to make improvements in availability, integrity, and robustness. By improving the other components of the TKS shown in Figure 1, we can increase the short-term stability and the timing integrity of the signal. At some additional cost (but still less than Block IIR), it is possible to ameliorate the effects of any remaining frequency breaks in the ERAFS. This should improve peak ERDs when these breaks occur and reduce Control Segment workload. Finally, the new TKS allows a new RAFS to be powered up and tested for timing stability before it is brought online.

We will describe the improved components and then describe how these building blocks can be combined to build a TKS with the desired cost and performance characteristics. But first, we need to explain why we need a TKS in the first place.

WHY NOT SIMPLIFY THE ORIGINAL TKS?

Figure 12 shows a block diagram for a simplified TKS in which the RAFS generates the baseband signal directly via a synthesizer. Such a scheme appears attractive, particularly as the requirement for SA becomes less important and in light of technology advances that have made synthesizers less expensive, more accurate, and rad-hard. The tuning commands could be generated either via hardware or software, and the phase meter would be used to aid integrity. Unfortunately, frequency errors or phase breaks of the RAFS reference cannot be detected reliably by such a scheme, since both inputs to the phase meter will be equally affected. We refer to non-detection of a significant frequency or phase jump of the TKS output as an *integrity failure*. The oversimplified TKS of Figure 12 is prone to integrity failures. Therefore, even though technology now allows accurate signal generation without a feedback loop, any design that bases the TKS output on a single oscillator has unacceptable integrity.

Another advantage of using two clocks in a feedback arrangement like Figure 1 is that the code clock can be designed for very high short-term stability, and the reference RAFS clock can be designed for very high long-term stability. The opposite extremes of either clock will not affect system performance. High short-term stability may be very important for space applications, time transfer, and specialized applications.

BUILDING BLOCK # 1 - ERAFS

The first building block of an improved TKS is the ERAFS. The improved performance of the ERAFS has already been described. Use of Xenon gas rather than krypton in the rubidium lamp, and other changes, should result in improved long-term stability and fewer frequencies breaks. Advanced digitally controlled Rb or Cs clocks and ion-pumped techniques also show promising features that are applicable to spac-segment GPS operation. These technologies can be integrated into the GPS architecture to further improve the stability of the GPS system.

BUILDING BLOCK # 2 – PRECISION PHASE METER (PPM)

The *precision phase meter* (PPM) is the second new building block. In Figure 1, the existing phase meter measures the phase of the reference epoch, which occurs every N_R cycles of the RAFS, to the timing of the X1 epoch, which occurs every 15,345,000 cycles of the *code clock* produced by the VCXO. The phase meter measures this phase with a resolution of ±1.67 ns. The rms error of the Block IIR phase meter is no better than 0.68 ns, more typically 0.8 ns. To meet the short-term Allan deviation specification of Block IIR, it is necessary to smooth phase errors over a time period of ~150 seconds with a second-order filter in order to generate frequency correction commands to the VCXO in Figure 1. Even so, the primary cause of short-term (< 100 seconds) timing instability in the Block IIR TKS is the phase meter. Any attempt to improve short-term stability would be nearly impossible with the existing phase meter. ITT has built and demonstrated a PPM with an rms measurement error of 0.8×10^{-12} seconds, about 1,000 times more accurate than the existing design. Resolution (quantization) is typically less than 10^{-14} seconds. The design and implementation of the PPM is covered by US Patent 6,441,601 B1.

A block diagram is shown in Figure 13, and Table 1 compares the two phase meters. The PPM was implemented using a Xilinx FPGA. Examining the block diagram (Figure 13), the PPM samples one or two digital clocks, Measured Clock 1 (MCLK1) and, optionally, Measured Clock 2 (MCLK2), at the edges (one or both) of a third clock, the Sampling Clock (SCLK). The circuitry for each of the measured clocks is nearly identical, and consists of a sampler that generates a bitstream, a counter circuit for the bitstream, and proprietary sample steering logic that guides each sample to one of several counters. An X1 epoch input synchronizes one or more measurements per epoch to the 1.5 s epoch in a GPS system. The counter values were gathered and transmitted to a PC using an RS232 interface implemented in the FPGA. The interface and processor would be different in a GPS implementation, but the computation required to calculate the phase is only a few comparisons, multiplications, and additions, which is insignificant compared to other TKS processing. The test setup is shown in Figure 14. Measurement accuracy tests from this test setup are shown in Figure 15 and Figure 16, and show that measurement accuracy ranges from 1.14 ps with a short 0.04-second measurement integration time to 0.64 ps with a 0.15-second integration time.

BUILDING BLOCK #3 – IMPROVED CODE CLOCK

This is the third building block of an improved TKS. ITT is evaluating the replacement of the VCXO used to generate the code clock in Block IIR with a combination of a stable oven-controlled fixed-frequency crystal oscillator (OCXO) and a digital synthesizer. Since an improved VCXO is needed to meet the short-term Allan deviation requirements of Figure 11, a redesign is needed anyway. If the OCXO had a similar Allan deviation to the IIR VCXO, the combination would likely be less expensive, more reliable, and use less power. Alternatively, a higher performance OCXO could be selected. As will be discussed, an OCXO with 50-second stability of 10^{-13} would allow RAFS frequency breaks larger than about 8×10^{-13} to be detected, characterized, and removed from the TKS before they affect the navigation signal. An OCXO with better long-term stability might be desired for other reasons.

CONCLUSIONS

The stable GPS IIR RAFS/TKS is yielding excellent navigation performance. We expect future GPS IIR SVs to yield performance that is comparable to the best of the existing on-orbit performance. The addition of GPS IIR continues to enhance GPS constellation. Replacing the RAFS with ERAFS and using the PPM will allow even greater performance gains. Various improvements in the TKS design will allow for better integrity and availability of the GPS signal to meet next-generation requirements.

ACKNOWLEDGMENTS

The data for Figure 2 WERE obtained from NIMA (National Imagery and Mapping Agency) at the Web site http://164.214.2.59/geospatial/products/GandG/sathtml/.

REFERENCES

[1] J. Vanier and L. G. Bernier, 1981, *"On the Signal-to-Noise Ratio and Short-Term Stability of Passive Rubidium Frequency Standards,"* **IEEE Transactions on Instrumentation and Measurement IM-30,** 277-282.

Table 1. Comparison of precision phase meter (PPM) to Block IIR phase meter.

	Block IIR Phase Meter	**Precision Phase Meter**
Typical accuracy (rms)	900×10^{-12} s	0.8×10^{-12} s
Measurement period	50-150 ms	~ 100 ms
Measurements/epoch	1	up to 15
Sensitivity to phase noise and squaring circuit noise	141%	< 1%
# Clocks compared	2	2 or 3
Additional & analog components?	600 MHz xtal oscillator Reference Epoch Generator RAFS switching components	3-input mode requires Sampling Clock oscillator
Continuous monitoring of reference clock and code clock?	No	Yes (coarse phase counters run continuously)

Table 2. Improving the Next-Generation GPS TKS.

NEXT GENERATION TKS IMPROVEMENT	**FACTORS CAUSING IMPROVEMENT**	**IMPROVEMENT REALIZED** (yellow: requires “tie-breaking” clock) (blue: requires 2nd powered RAFS)
Short-term (< 300 s) Allan deviation	1000:1 improvement in phase meter accuracy	Phase meter noise in TKS output reduced by factor of 10 even with 10 s time constant
	Improved ST stability of OCXO / synthesizer combination	10× improvement possible, depending on OCXO Allan deviation at $\tau < 30$ s
Medium-term (300 – 30,000 s) Allan deviation	ERAFS – 3 to 4x better stability across range	
	Contribution of orbital temperature variation reduced because of short time constant	Reduced from 3×10^{-14} (most significant factor at ¼ day) to 3×10^{-15} (insignificant)
	IIR RAFS already exceeds spec by 2-4×	10× improvement achievable vs. IIR spec
Long-term Allan deviation	ERAFS – expect improvement of at least 2× based on improved S/N ratio, 2-3× based on Fig. 11	ERAFS performance flows through to system performance
	IIR RAFS already exceeds spec by 2-4× (except SN 009, Fig. 7)	10× improvement achievable vs. IIR spec
Robustness	Shorter TKS time constant means TKS output affected less by VCXO/OCXO instabilities	10× reduction in ERD caused by a given anomaly.
	ERAFS – improved design of rubidium lamp	RAFS frequency breaks that affect ERDs will be ~50% less frequent
	PPM is accurate enough to isolate and correct RAFS frequency breaks if optional clock of Fig. 18 has high short-term stability	ERDs won’t be affected by the worst of the remaining frequency breaks
Integrity	PPM monitors 10.23 and RAFS output continuously	Short-term interruptions much more likely to be detected, especially use 3 inputs of PPM With CPU or PPM enhancement, faster fault detection
	PPM has ability to compare 3 clocks	Very likely that either a single or dual simultaneous error would be detected
Availability	PPM accuracy allows frequency difference of two RAFS to be measured	Possible to measure backup RAFS frequency before switching to it
	TKS design using all “tie-breaker” clock can correct clock errors	No need to deny signal using NSC for most clock errors

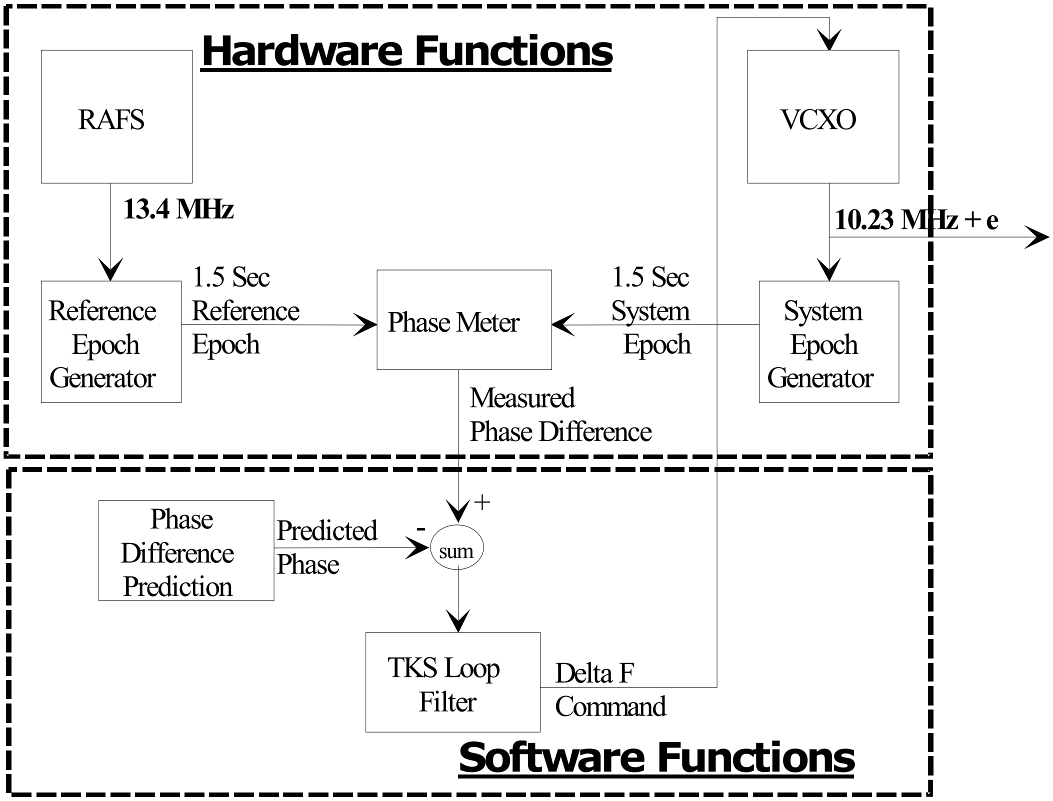

Figure 1. TKS block diagram.

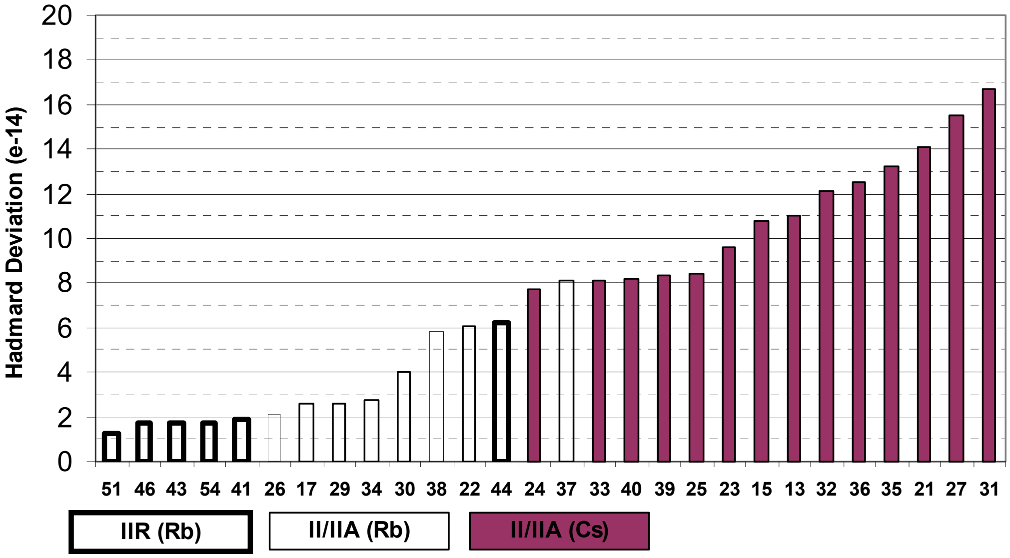

Figure 2. Ranking of GPS clocks by Hadamard deviation at 1 day (Q1-2002).

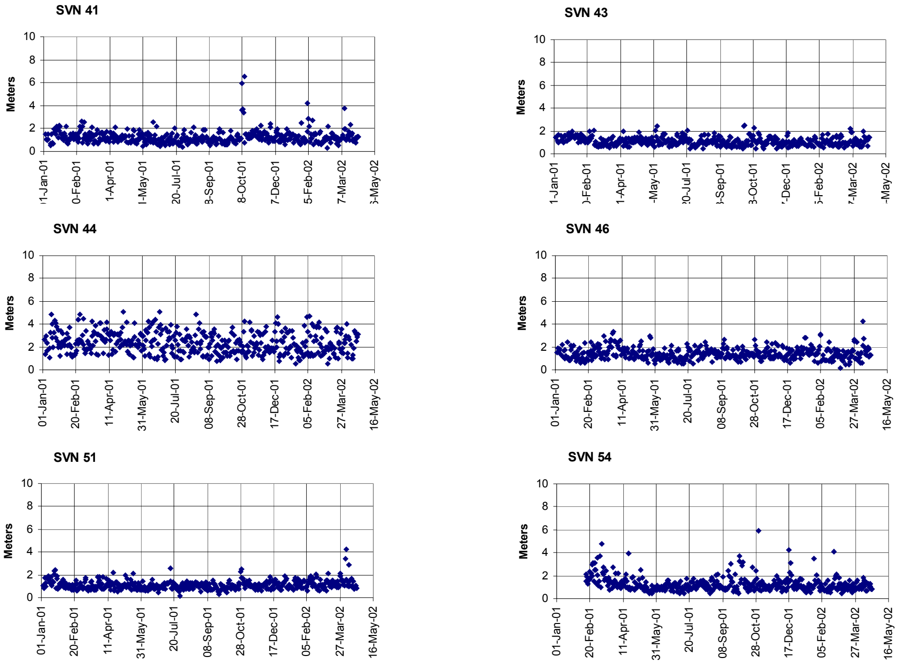

Figure 3. GPS IIR ERD January 2001 through April 2002.

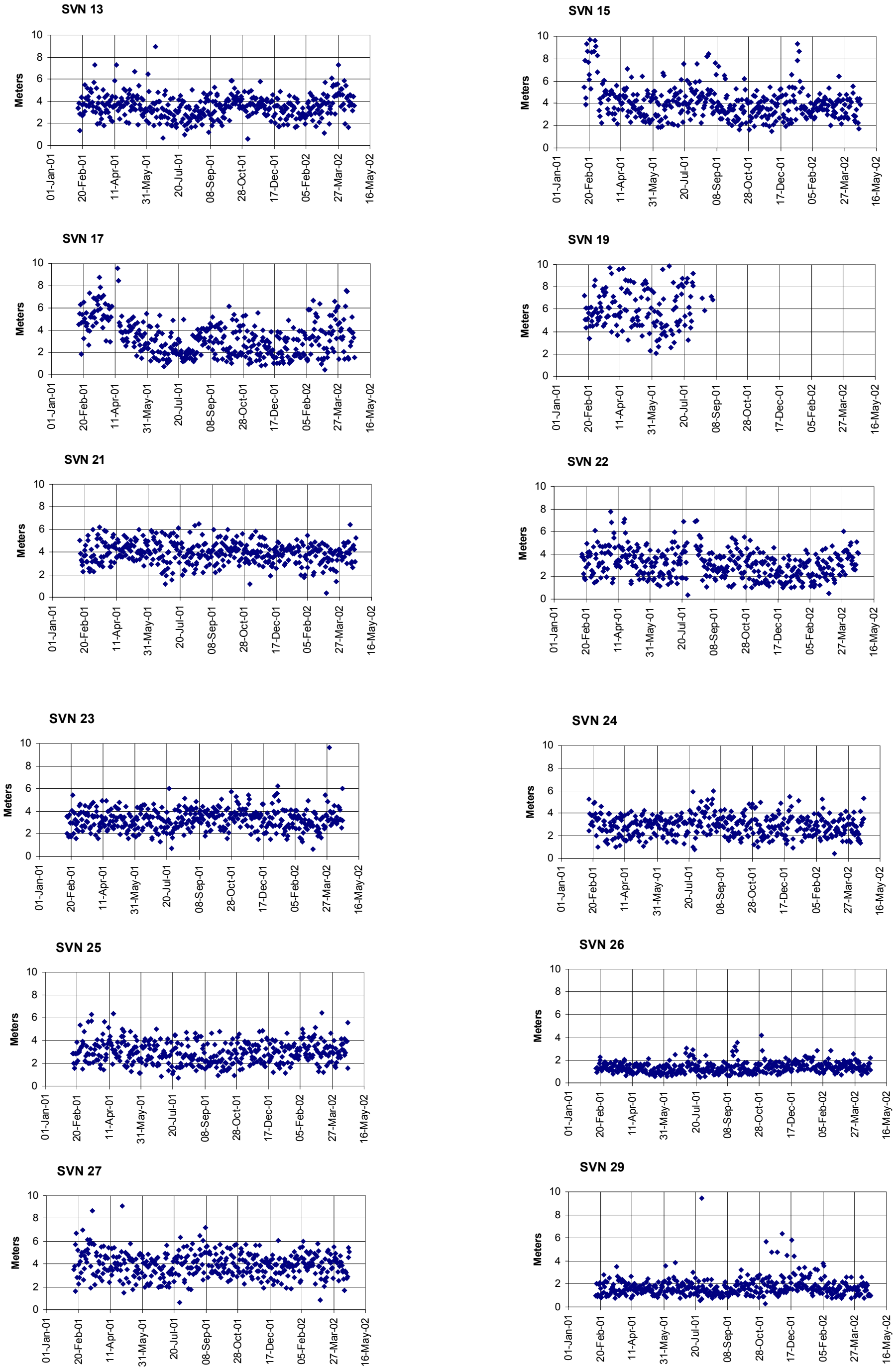

Figure 4. GPS II/IIA ERD January 2001 through April 2002.

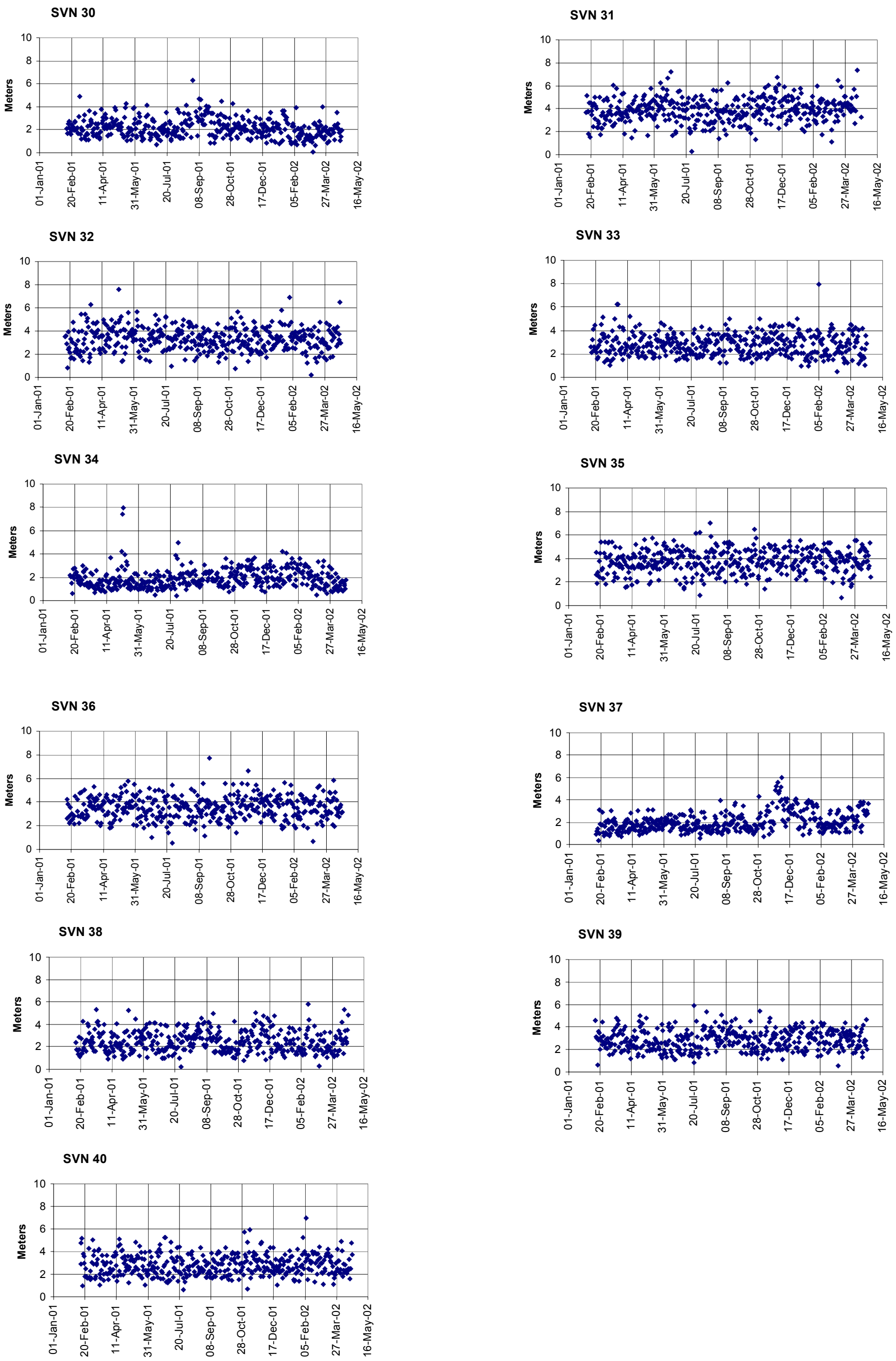

Figure 5. GPS II/IIA ERD January 2001 through April 2002 (continued).

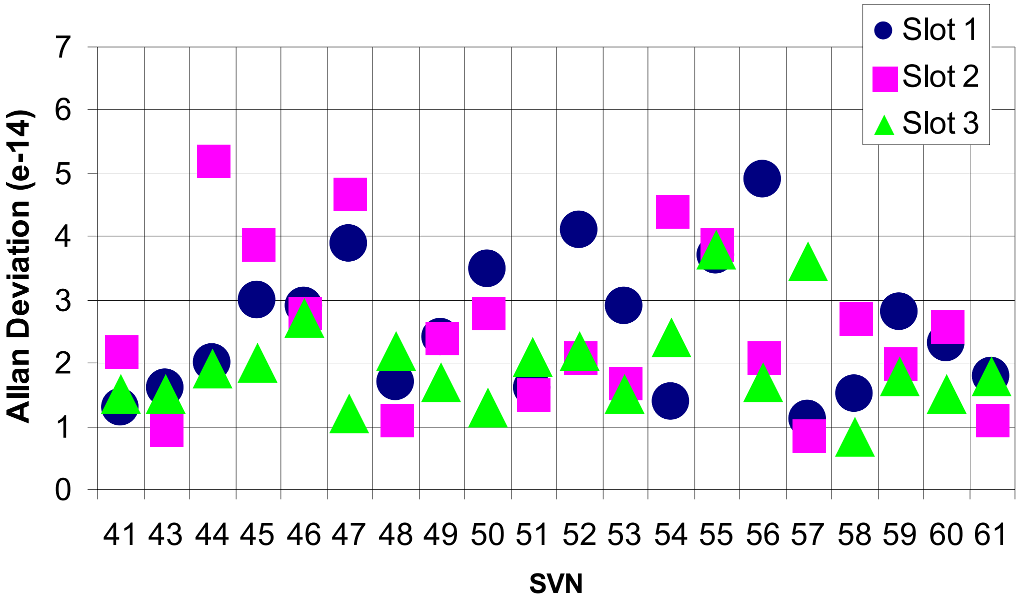

Figure 6. GPS IIR factory-measured frequency stability at 1 day.

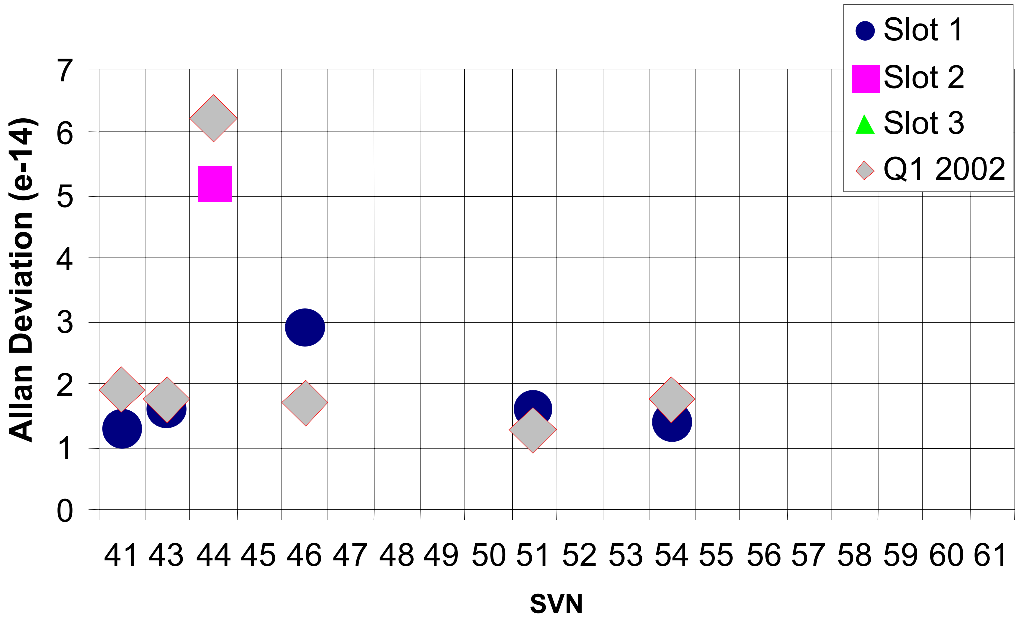

Figure 7. GPS IIR comparison of factory to on-orbit frequency stability.

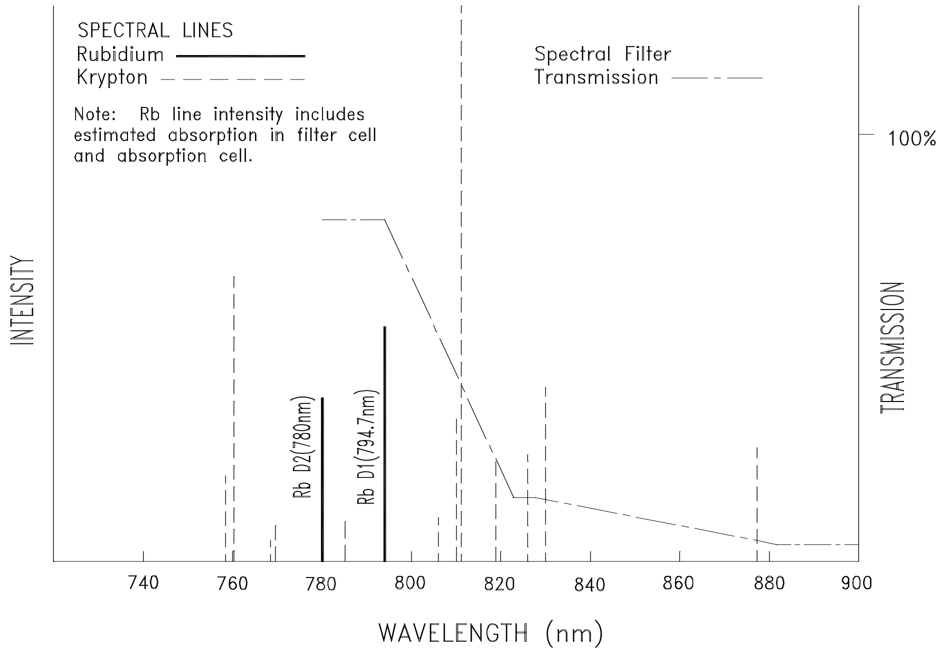

Figure 8. Krypton buffer gas lamp spectrum and spectral filter characteristic.

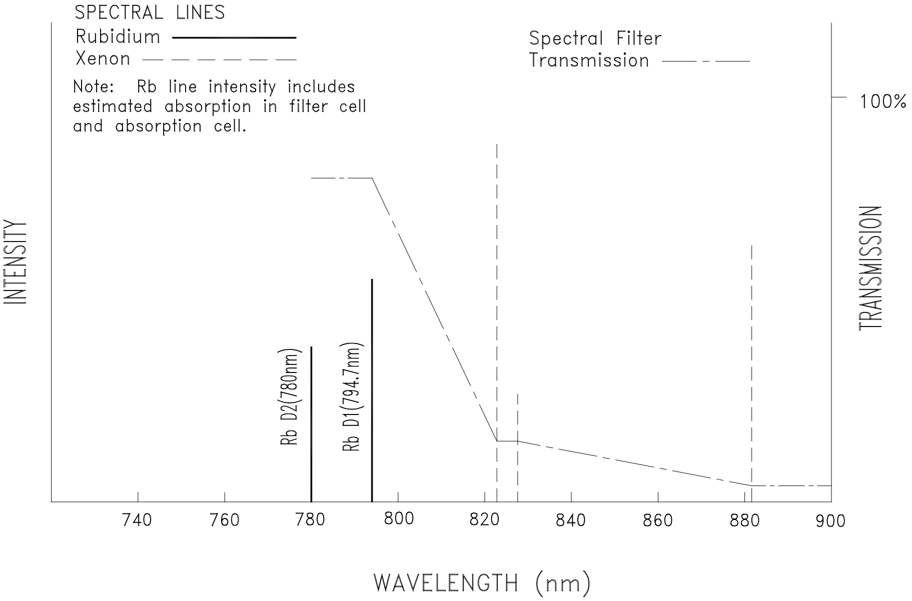

Figure 9. Xenon buffer gas lamp spectrum and spectral filter characteristic.

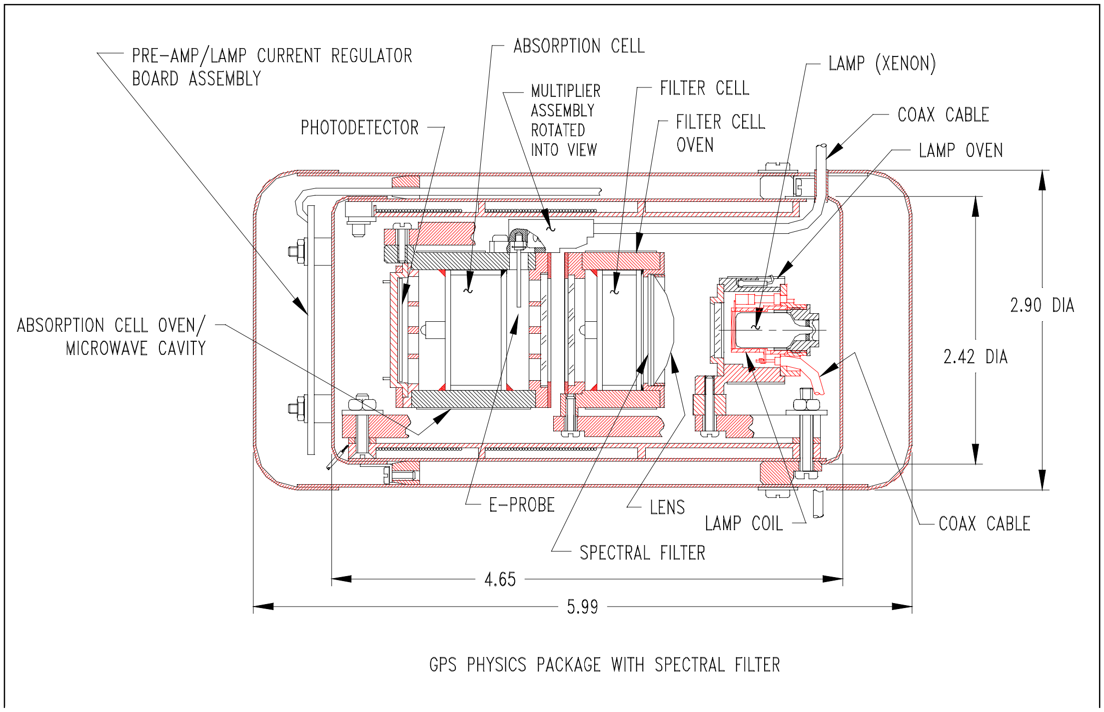

Figure 10. PerkinElmer physics package.

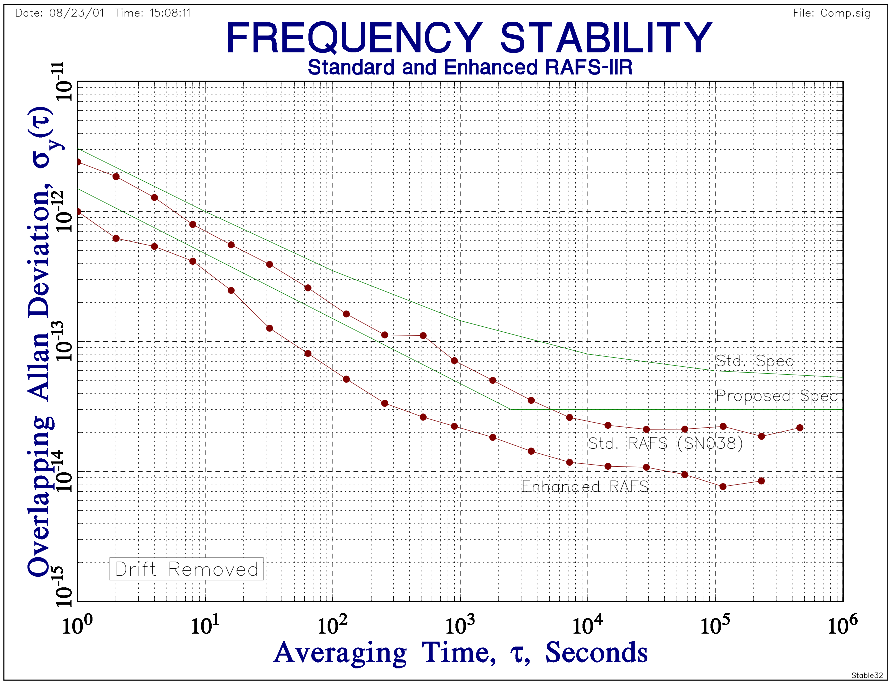

Figure 11. Standard RAFS and specification vs. ERAFS and proposed specification.

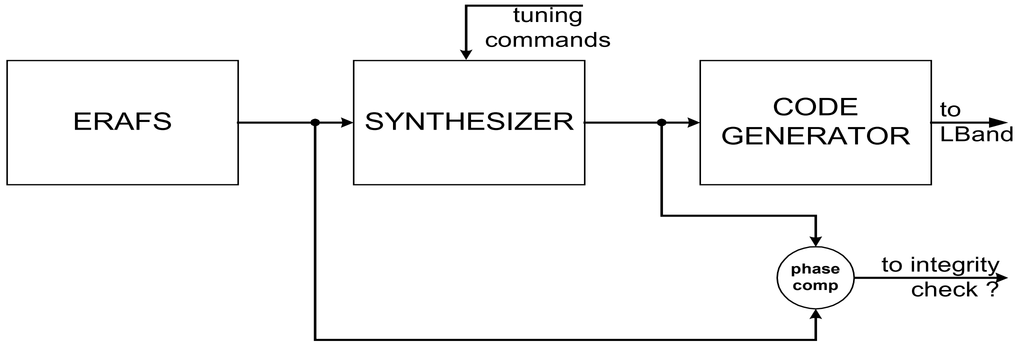

Figure 12. TKS design without independent reference, code generator oscillators.

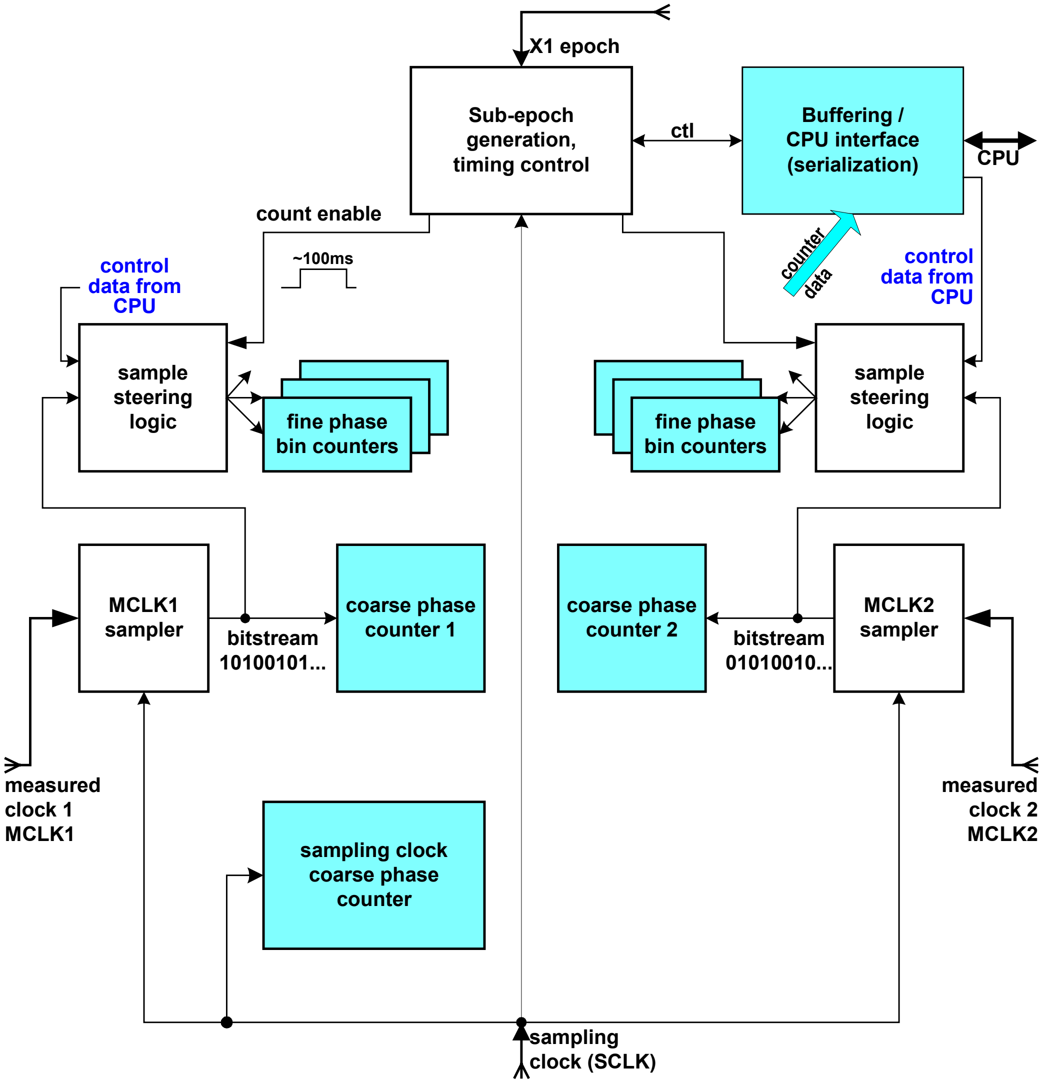

Figure 13. Precision phase meter (PPM) block diagram (US Pat. 6,441,601 B1).

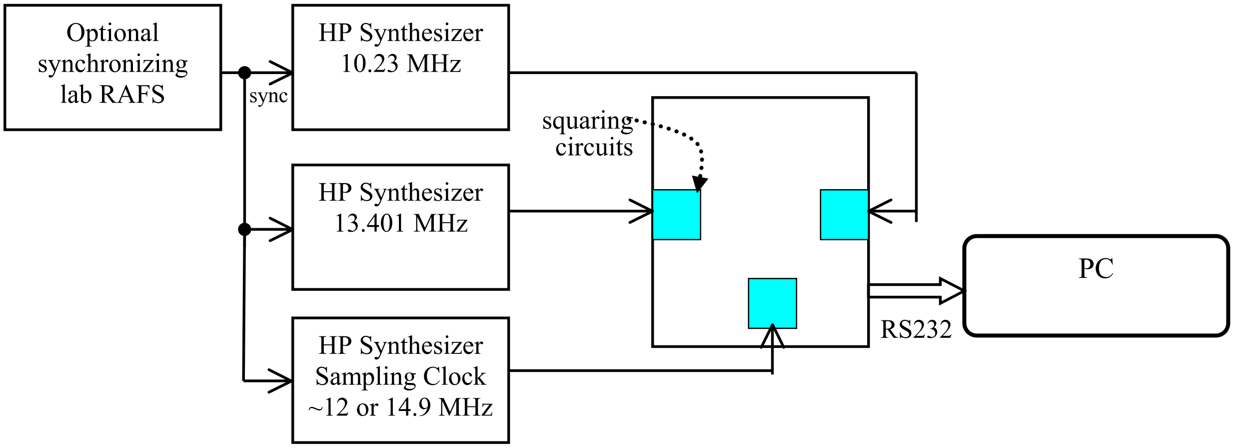

Figure 14. Precision phase meter evaluation test setup.

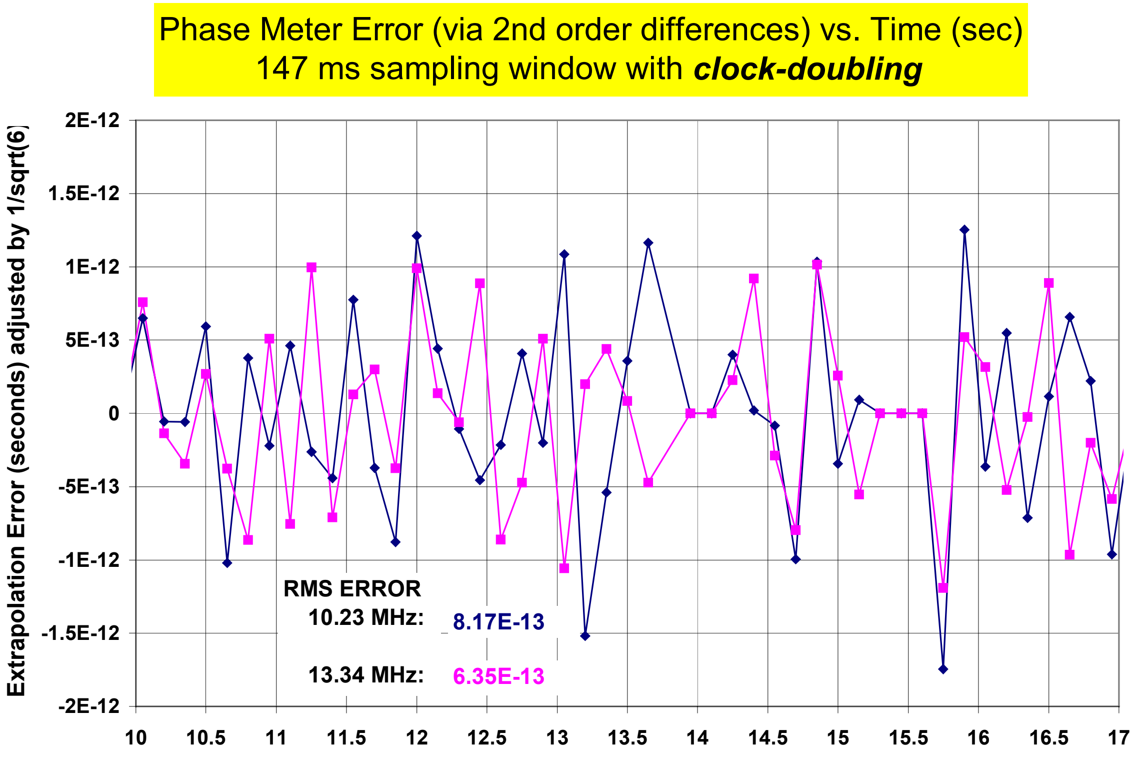

Figure 15. PPM rms error measurement with 0.147 s integration time.

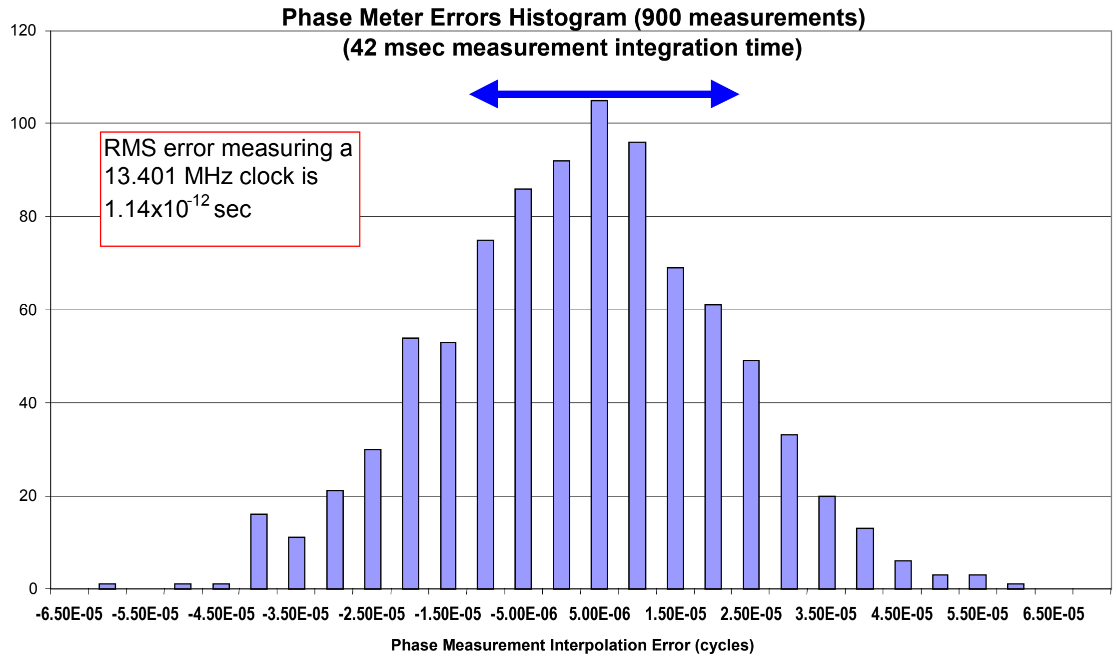

Figure 16. PPM error histogram in cycles, short integration time.

QUESTIONS AND ANSWERS

MICHAEL GARVEY (Symmetricom): It is okay if you defer this question, but I think something that sits in the minds of a lot of us is why did the original TKS not use some heterodyne technique to reduce the noise? An obvious thing would be to mix the clock with the oscillator and get maybe a factor of 3 or 4.

TODD DASS: I will defer the question. I know a lot of the original design decisions were driven by the RAD-hardness requirement.

JIM DeYOUNG (U.S. Naval Research Laboratory): For the second author, I was somewhat surprised you said you put the filter in for the krypton light, and why you cannot filter out the left side impurities which, I presume, are on the bluer side. And also, are these just standard glass filters? So you should be able to filter out the left side also.

JOHN VACCARO: They are interference filters; they add glass for the coating. I guess it is because it is just a lot easier with the xenon lamp to have all the spectral lines on one side. You put a low-pass filter rather have some kind of band-pass filter for the krypton lamp. There are a lot of details on how well the filters work. When you try to get a narrow pass band, you run into some problems on the angles of the lights coming in and so forth. So it just works much nicer with the xenon lamp.